HAL
open science

New Intermediate Polymorph of 1-Fluoro-adamantane and Its Second-Order-like Transition toward the Low Temperature Phase

Lina Yuan, Simon Clevers, Antoine Burel, Philippe Négrier, Maria Del Barrio, Bacem Ben Hassine, Denise Mondieig, Valérie Dupray, Josep Ll Tamarit, Gérard Coquerel

To cite this version:

Lina Yuan, Simon Clevers, Antoine Burel, Philippe Négrier, Maria Del Barrio, et al.. New Intermediate Polymorph of 1-Fluoro-adamantane and Its Second-Order-like Transition toward the Low Temperature Phase. Crystal Growth & Design, 2017, 17 (6), pp.3395-3401. 10.1021/acs.cgd.7b00353 . hal-01551454

HAL Id: hal-01551454

https://hal.science/hal-01551454v1

Submitted on 30 Jun 2017

HAL is a multi-disciplinary open access archive for the deposit and dissemination of scientific research documents, whether they are published or not. The documents may come from teaching and research institutions in France or abroad, or from public or private research centers.

L'archive ouverte pluridisciplinaire **HAL**, est destinée au dépôt et à la diffusion de documents scientifiques de niveau recherche, publiés ou non, émanant des établissements d'enseignement et de recherche français ou étrangers, des laboratoires publics ou privés.

Distributed under a Creative Commons Attribution - NonCommercial - ShareAlike 4.0 International License

New Intermediate Polymorph of 1-Fluoro-adamantane and Its Second-Order-like Transition toward the Low Temperature Phase

Published as part of a Crystal Growth and Design virtual special issue of selected papers presented at the 12th International Workshop on the Crystal Growth of Organic Materials (CGOM12 Leeds, UK)

Lina Yuan,[†] Simon Clevers,[†] Antoine Burel,[†] Philippe Negrier,[‡] Maria del Barrio,[§] Bacem Ben Hassine,[‡,§] Denise Mondieig,[‡] Valérie Dupray,[†] Josep Ll. Tamarit,[§] and Gérard Coquerel*[,†]

[†]Normandie Université, Laboratoire SMS EA3233, Université de Rouen, F 76821, Mont Saint Aignan, France

[‡]LOMA, UMR 5798, CNRS, Université de Bordeaux, F 33400 Talence, France

[§]Grup de Caracterització de Materials, Department de Física, EEBE, Campus Diagonal Besòs, Eduard Maristany, 10 14, Universitat Politècnica de Catalunya, 08019 Barcelona, Catalonia, Spain

ABSTRACT: Phase transitions of 1 fluoro adamantane have been thoroughly investigated by temperature resolved second harmonic generation (TR SHG) and X ray powder diffraction (XRPD). A new polymorph—an intermediate centrosymmetric phase (MT)—between the known orientationally disordered high temperature phase (HT, $Fm3m$, $Z = 4$) and the low temperature phase (LT, $P42_1c$, $Z = 2$) was unveiled by TR SHG. The crystal structure of MT was resolved by XRPD in the $P4_2/nmc$ ($Z = 2$) space group, and it is related to the LT phase in a group−subgroup relation. No evidence of any solid−solid transition between these two phases by differential scanning calorimetry (DSC) or cold stage microscopy could be obtained. Therefore, combing TR SHG, XRPD, DSC, and cold stage microscopy results, a second order transition mechanism is proposed for the MT ↔ LT transition. Moreover, the critical exponent (β) of the order parameter was calculated by fitting TR SHG data to a critical power law. The obtained β value (0.26) is close to the value from XRPD data (0.25).

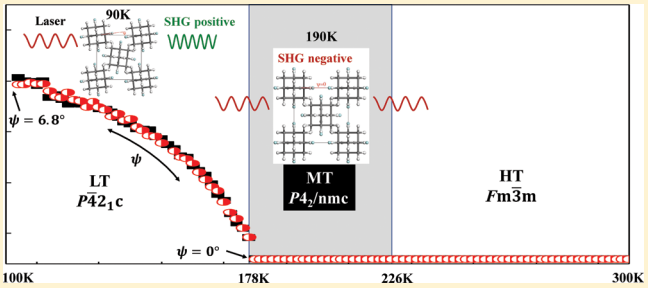

INTRODUCTION

Diamondoids formed by carbon cages have received much interest, in particular, for building up organic crystals with large cavities and specific physical and chemical properties.[1−5] The simplest diamondoids, adamantane and its derivatives, exhibit an orientationally disordered (OD) phase (plastic phase) and show rich polymorphic transitions upon temperature or pressure changes.[6−11] 1 Fluoro adamantane (1 F A hereafter, Figure 1) is one of the 1 substituted adamantanes, and thus far, two polymorphs have been revealed: one OD phase at high temperature (HT) and a less disordered low temperature (LT) phase.

The phase transition HT ↔ LT was first detected by differential scanning calorimetry (DSC) at 222 K (upon heating) with an enthalpy of 1.5 kJ/mol.[12] Later, Kawai et al.[13] reported the transition occurs at 227 K with an enthalpy of 1.7 kJ/mol upon cooling and at 231 K with an enthalpy of 1.6 kJ/mol upon heating. The transition displays a hysteresis which indicates a first order behavior in the Ehrenfest classification.[14] The HT phase has been widely studied by thermal analysis,[12] X ray diffraction,[15] NMR,[8] single crystal Raman scattering,[16] dielectric analysis,[17] and incoherent quasi elastic neutron scattering.[18] The structure of the HT phase was determined as face centered cubic ($Fm3m$) by single crystal X ray diffraction[15] and by X ray powder diffraction (XRPD).[19] However, less was known about the LT phase before the recent publication by Ben Hassine et al.,[19] in which was reported the resolution of the crystal structure of the LT phase at 100 K by XRPD in the tetragonal noncentrosymmetric $P42_1c$

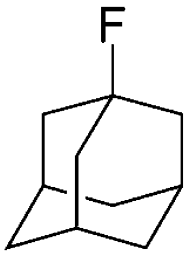

Figure 1. Molecular structure of 1 fluoro adamantane (1 F A).

space group (Z = 2)—CCDC number 1455093.[19] The variation of cell parameters and the cell volume of 1 F A were also monitored by temperature resolved XRPD from 90 K to 360 K, and a sole discontinuity of the lattice parameters across the HT ↔ LT transition was observed. Based on these results, it was presumed in the work of Ben Hassine et al.[19] that only two polymorphs exist and, consequently, that the structure of 1 F A could be resolved in the $P42_1c$ space group from 90 K until the phase transition toward the HT phase. As the LT polymorph is still disordered (as assessed by NMR and BDS[8,19]), 1 F A is a perfect candidate to go deeper into the study of molecular motions in the solid states and across polymorphic transitions.

In this mater, temperature resolved second harmonic generation (TR SHG) can be used to gather valuable information. SHG (second harmonic generation) refers to an optical process in which an electromagnetic wave gives rise to a new wave at half the initial wavelength while traveling through a noncentrosymmetric material.[20−25] The variation of the second harmonic (SH) signal versus temperature can be obtained by TR SHG. Vogt[26,27] detailed that the temperature dependence of higher rank tensors describing SHG is related to variations of long and short range order. Moreover, Dougherty and Kurtz[21] mentioned that dynamic disorder possibly couples with local polarization fluctuations and then can induce modification in the SH signal. These make TR SHG a useful tool to detect phase transitions and polymorphs for systems involving symmetry changes in crystalline structures and molecular motions in noncentrosymmetric crystalline phases. TR SHG has already been applied to monitor transitions between monotropically or enantiotropically related solid phases,[28−31] and to track ferroelectric−paraelectric phase transitions[32,33] and order−disorder phase transitions[27,34,35] with as a required condition that at least one noncentrosymmetric crystalline structure is involved.[20,21,36−39]

In 1 F A, the HT phase is centrosymmetric and consequently generates no SH signal. The LT phase resolved in a noncentrosymmetric space group generates a SH signal. Thus, the phase transition between the HT phase and the LT phase can be studied by TR SHG. Through a careful investigation of phase transitions in 1 F A (especially at low temperatures) by the synergistic approach of combining TR SHG and XRPD, not only a new polymorph was ascertained in this work but also the knowledge on the mechanism of ordered−disordered transitions was improved.

■ EXPERIMENTAL SECTION

Materials. 1 Fluoro adamantane (CAS registry number: 768 92 3) was purchased from ABCR in Germany (98.3% purity, 1.7% impurity of 1 adamantanol). Crystals used in this work were purified by recrystallization from methanol (HPLC grade), and the average crystal size was 200 μm. The purity was checked by GC MS (higher than 99.9%). See SI 1: (a) the purification procedure of commercial 1 F A and (b) the purity checking process by GC MS.

Methods. *Temperature-Resolved Second Harmonic Generation (TR-SHG).* The nonlinear optical method has been introduced in our previous papers.[28,34,40−43] Powder sample (50 mg) was placed in a computer controlled thermal stage (Linkam THMS 600). The sample was scanned at 1 K/min between 100 and 293 K. The number and the duration of the TR SHG analyses were chosen to ensure the best stability of the laser beam and the best stability of the compound under the laser irradiation. Therefore, the points on the TR SHG curve were recorded every 2 K and each point corresponds to the average value of the SH signal recorded over 3 s (the temperature variation during the recording is 0.05 K). For each SH signal versus temperature plot, the SH data were normalized using the maximum SH intensity, which was obtained by fitting the SH curve of the raw values.

The SH intensity generated by a given sample depends on numerous parameters (molecular nature, quality of the long range order, i.e. the crystallinity, crystal structures, size, and orientation of the crystals).[20,21] Therefore, in order to get reproducible results, we ensured that the laser irradiates the same area of the sample (40 mm^2) all along the experiments. The standard deviation of the SH signal was estimated to be ca. 3%, which is mainly due to energy fluctuations of the laser beams.

Differential Scanning Calorimetry (DSC). Thermal analyses were conducted in a Netzsch 204 F_1 DSC apparatus equipped with liquid nitrogen as the coolant. Both the temperature and the enthalpy changes of the calorimeter were calibrated by using the phase transition of cyclohexane and mercury. Samples with a mass of ca. 8 mg (with a maximum deviation of 0.05 mg) were sealed in a 25 μL aluminum crucible. Thermograms were obtained at a scanning rate of 1 K/min. The atmosphere during the measurements was regulated by a nitrogen flux (40 mL/min). Data treatment was performed with Netzsch TA Proteus V4.8.4 software.

Cold-Stage Microscope. Samples were loaded into an amorphous quartz crucible and set in a THMS 600 temperature stage setup (Linkam, the same as that used in TR SHG method). Liquid nitrogen was used as the coolant, and the nitrogen flux was regulated via an automatic pump. The setup was coupled with a Nikon Eclipse LV100 microscope and connected to a computer for image captures by a CCD camera.

Note that the temperature accuracy of the Linkam at low temperatures was checked. The melting points of *o* xylene (249 K) and tetrahydrofuran (165 K) in HPLC grade were observed by cold stage microscope. Different heating/cooling rates were used (0.5 K/min, 1 K/min, 2 K/min, 4 and 5 K/min) and compared with DSC results. The temperature difference between cold stage microscopy and DSC was observed to be lower than 1 K.

Curve Fitting. Data were fitted to specific expressions by application of the Levenberg−Marquardt (least squares method) algorithm using the program Origin 10.

X-ray Powder Diffraction (XRPD). X ray powder diffraction data were collected by means of a horizontally mounted INEL cylindrical position sensitive detector (CPS 120) to pursue a careful structural determination from the HT to LT phases. The detector constituted by 4096 channels was used in Debye−Scherrer geometry. External calibration using the $Na_2Ca_2Al_2F_{14}$ (NAC) cubic phase mixed with silver behenate was performed by means of cubic spline fittings providing an angular step of 0.029° (2θ) between 4° and 120°. Monochromatic Cu Kα1 radiation (λ = 1.5406 Å) was selected with an asymmetric focusing incident beam curved quartz monochromator. The samples were introduced into 0.5 mm diameter Lindemann capillaries which were rotated perpendicular to the X ray beam direction in order to decrease as much as possible the effects of preferred orientations. Temperature was controlled with an accuracy of 0.1K by means of a liquid nitrogen 600 series cryostream cooler from Oxford Cryosystems.

■ RESULTS AND DISCUSSION

Characterization of 1-F-A Phase Transitions by DSC. A single detectable thermal event was observed by DSC between 120 and 300 K for a heating rate of 1 K/min (Figure 2). Upon cooling, the onset temperature is 226.0 ± 0.3 K with an enthalpy of 1.9 ± 0.1 kJ/mol. Upon heating, a hysteresis is observed, with an onset temperature at 231.0 ± 0.2 K and an enthalpy of 1.8 ± 0.1 kJ/mol. This thermal event obviously corresponds to a first order phase transition. These values are consistent with previously reported values from the literature.[12,13,19] Note that the use of a higher heating rate (5 K/min) led to a similar result (see SI 2).

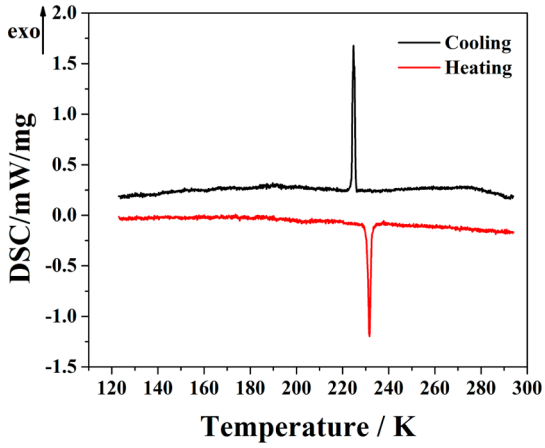

Figure 2. DSC measuring curves obtained for the phase transitions of 1 F A. Black line, upon cooling (1 K/min); red line, upon heating (1 K/min).

TR-SHG Measurements. It is first necessary to mention that, in the present case, the intensity of the measured SH signal can be generated only by the noncentrosymmetric crystalline LT phase of 1 F A. Based on Kurtz and Perry,[20] SH intensity can be considered proportional to the mass fraction (or molar fraction) of the LT phase.

The thermal evolution of 1 F A was monitored by TR SHG through tracking the SH signal generated by the LT phase versus temperature (Figure 3).

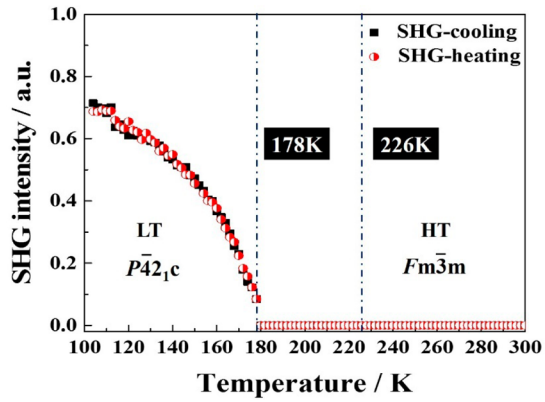

Figure 3. TR SHG curves obtained for the phase transition of 1 F A. Black square, upon cooling (1 K/min); red spot, upon heating (1 K/min). The signal appears/disappears at 178 K and increases with lowering the temperature down to 100 K.

Apparently, the sample exhibits a positive SH signal at 100 K, which proves the structure is noncentrosymmetric at this low temperature and confirms the reliability of the XRPD crystal structure determination.[19]

Surprisingly, the SH signal was observed to appear only at 178 K (upon cooling) while the transition temperature was detected at 226 K by DSC (black curve in Figure 2). The temperature difference is 48 K. Obviously, this difference is too large to be caused by the thermal gradient between the sample and the heating plate. Possible reasons for this phenomenon were investigated. First, we supposed that the SH signal generated by 1 F A between 178 and 226 K could have fallen under the detection threshold. Even though the detection threshold of our TR SHG apparatus can be considered as good (evaluated at ca. 1/100 compared to the SH intensity of the quartz standard, 45 μm), the sample was annealed at 213 K, a temperature between 178 and 226 K in order to obtain a better crystallization of the sample (i.e., to possibly enhance the SH signal). After 10 h, no SH signal was detected (see SI 3), which strongly suggests that no LT phase crystallized in the range of 178 and 226 K. Second, it was supposed that the transition kinetics might be low and the thermodynamic equilibrium was not reached in this temperature range. So, the sample was annealed at 167 K to possibly reach the thermodynamic equilibrium. Nevertheless, after 10 h, no variation of the SH signal was observed, indicating that the maximum amount of LT phase was already reached under the conditions used for the TR SHG experiments (see SI 4).

Finally, these results led us to envisage that 1 F A exhibits an intermediate phase between the HT and LT phases in the temperature range 178 K to 226 K. In the following, this intermediate phase is referred to as MT (for medium temperature). Since no SH signal was detected between 178 and 226 K, the MT phase probably exhibits a centrosymmetric crystalline structure (confidence higher than 99%[36]).

Another interesting result is that no hysteresis was observed for the SH signal upon heating and cooling. That is to say, the SH intensity profile is thus completely reversible (i.e., thermal cycles after cycles or after stopping and restarting the heating/cooling process). Consequently, a second order transition between MT ↔ LT can be suspected, complementary with the following observations:

(i) no detectable enthalpy change detected by DSC around 178 K;
(ii) no transition front propagation observed by cold stage microscope (see SI 5);
(iii) no change of the cell volume at the presumed transition temperature (178 K) in the work of Ben Hassine et al.[19]

A thorough reinvestigation of the structures resolved from XRPD at various low temperatures confirmed this hypothesis as described in the following.

Crystal Structure of MT Phase Determined from XRPD. When cooling down from HT phase to the LT phase, single crystals break, and thus, powder diffraction is the only way to determine the structure of the low temperature phases. Therefore, powder X ray patterns obtained at 90 K and 190 K were submitted to a Rietveld refinement,[44] with the same rigid body constraints that are depicted in the work of Ben Hassine et al.[19] A single overall isotropic displacement parameter and preferred orientation by using the Rietveld−Toraya function were refined. The final refined patterns together with the experimental and refined pattern differences are shown in Figure 4. The Rietveld refinement converged for the LT phase and the MT phase to a final R_{wp} value of 6.60% and 6.32%, respectively. The determined crystallographic data of both phases are summarized in Table 1.

A crystal structure validation by Platon[45] was performed on the two resolved space groups. For the LT crystal structure at 90 K, Platon results showed that no space group change is needed. While, if the MT phase is resolved in the space group of the LT phase (at 190 K), missed or additional symmetry is reported and Platon suggested the space group of $P4_2/nmc$. These results proved that the resolutions of the space group in the MT and LT phases are robust.

Mechanism of the MT ↔ LT Phase Transition. The presumed second order phase transition of MT ↔ LT can be

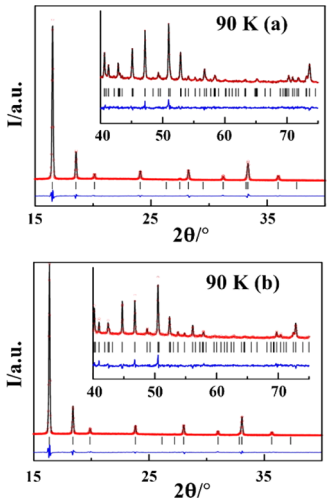

Figure 4. Experimental (red circles) and Rietveld refined (black line) diffraction patterns along with the difference profile (blue line) and Bragg reflections (vertical black sticks) of (a) the LT phase at 90 K and the (b) MT phase at 190 K. The insets show the high angle portion of each pattern (scaled to enhance their visibility).

Table 1. Crystallographic Data Determined for the MT Phase and the LT Phase

	MT phase	LT phase
temperature (K)	190	90
crystal system	tetragonal	tetragonal
space group	$P4_2/nmc$	$P\bar{4}2_1c$
$a = b$ (Å)	6.8145 (5)	6.7696 (4)
c (Å)	8.9232 (9)	8.8211 (9)
Z	2	2
volume (Å^3)	414.37 (7)	404.25 (6)
density (g/cm^3)	1.236	1.267

confirmed and interpreted microscopically by means of analysis of thermally induced structural changes. The structure of the LT phase is shown in Figure 5(a). The angle (ψ) defined

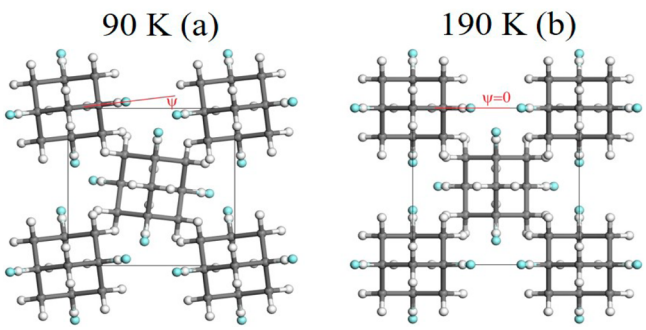

Figure 5. Crystal structure of 1 F A: (a) LT phase ($P42_1c$, $Z = 2$) at 90 K and (b) MT phase ($P4_2/nmc$, $Z = 2$) at 190 K. The fractional occupancy of 1/4 of the fluorine atoms (blue) remains unchanged across the MT ↔ LT transition.

between the C−F bond of the four equilibrium positions for the statistically disordered fluorine atoms (i.e., the molecular dipole direction) with the a (or b) tetragonal axis is ca. 6.8° at 90 K. Increasing the temperature, such angle continuously decreases, and at ca. 180 K, it vanishes and remains null until the phase transition to the HT phase. Such changes provide two new mirror planes perpendicular to the a and b tetragonal axes. Thus, the noncentrosymmetric space group $P42_1c$ ($Z = 2$) transforms to the centrosymmetric space group $P4_2/nmc$ ($Z = 2$), giving rise to the so called MT phase, which represents a group−subgroup transition. In addition, lattice parameters as well as volume as a function of temperature do not show any discontinuity (see SI 6). Therefore, the group−subgroup relation, the continuity of the lattice parameters and volume through the LT to the MT phase transition are in agreement with the continuity of the dynamic properties across this second order phase transition.[19]

Figure 5(b) depicts a structural projection of the MT phase along the c plane at 190 K. It is worth noting that the fractional occupancy of 1/4 of the fluorine atoms remains unchanged across the group−subgroup transition (MT ↔ LT). Therefore, it is probable that the phase transition does not change the type of molecular reorientation and that the dynamics and frequency of molecular motions in the solid state are not (or slightly) modified at the transition temperature (178 K). This could be an explanation of why this group−subgroup transition was not highlighted by other techniques such as BDS or solid state NMR.[8,19]

To summarize, at 178 K, a second order transition from the MT to the LT phase starts by a tilt of the angle ψ, resulting in an immediate change in the crystal structure. Then this angle ψ increases continuously with decreasing temperature but the crystal structure remains in the LT phase. The above explanations fit well with the TR SHG results. In Figure 3, the SH signal increases continuously from 178 to 100 K. Because SHG is intrinsically related to the crystal structure and molecular fluctuations,[36] it suggests that each SH signal corresponds to a LT form in which 1 F A molecules are tilted at a certain angle (e.g., $\psi = 6.8°$ at 90 K) by thermal agitation.

Variation of the Order Parameter with Temperature. The order parameter η describes the extent of order or disorder in a material. It is equal to unity in the perfectly ordered state and zero in the completely disordered state.[46]

TR SHG was used to track the variation of the order parameter η (according to the Landau theory) versus temperature and to determine the critical exponent β characteristic of this variation.

The temperature dependence of the SH intensity can be expressed as[47]

$$I_{\mathrm{SHG}}(T) \propto (\chi^{(2)}(T))^2 \left[\frac{l^2(T)}{n_1^2(T) n_2(T)} \cdot \frac{\sin^2(\delta(T))}{(\delta(T))^2} \right] \quad (1)$$

where l is the thickness of the crystals, and n_1 and n_2 are the indices of refraction for $\lambda_1 = 1.064$ μm (fundamental beam) and $\lambda_2 = 0.532$ μm (second harmonic beam), respectively. $\chi^{(2)}$ is the nonlinear susceptibility tensor, and $\delta = \frac{\pi l}{2 l_c}$ with the coherence length $l_c = \frac{\lambda_1}{4|n_1 - n_2|}$.

The term within brackets in eq 1 is generally responsible for a sin square modulation (sin c^2) of the SH intensity for single crystals. Considering that, for powders, the orientations of the crystals are random (averaging over all crystallographic directions) and the particle size (mean value ca. 200 μm in the present study) is likely to exceed the coherence length,[20] this modulation term can be neglected. Thus, in the following, we assume that the SH intensity is proportional to $(\chi^{(2)}(T))^2$. $\chi^{(2)}(T)$ is a third rank tensor with 27 coefficients, but the number of independent coefficients can be reduced to 3 in the

crystal class 42m by symmetry considerations. Moreover, assuming Kleinman conditions[48] are valid (no dispersion and absorption), the number of independent coefficients of the susceptibility tensor can be reduced to only one (d_{14} in the current case) and $\chi^{(2)}(T)$ can be expressed as (in the contracted notation):[49,50]

$$\chi^{(2)}(T) = 2\begin{bmatrix} 0 & 0 & 0 & d_{14} & 0 & 0 \\ 0 & 0 & 0 & 0 & d_{14} & 0 \\ 0 & 0 & 0 & 0 & 0 & d_{14} \end{bmatrix}$$

Taking into account the previous simplifications, $I_{SHG}(T)$ can be considered proportional to $d_{eff}^2(T)$, where d_{eff} is the effective coefficient of the nonlinear susceptibility. In the present case, d_{eff} is proportional to the d_{14} coefficient (using Voigt's convention).[51]

Moreover, d_{14} has already been shown to be a linear function of the order parameter η_{SHG}[35,36] in single crystals. In the present study, measurements are performed on powder samples with random crystallographic orientations, but that does not modify the fact that $\chi^{(2)}(T)$ depends only on one coefficient. Therefore, we can assume that the SH signal variations will be the same in all crystallographic directions. Hence, the square root of the SH intensity can be taken as an order parameter:

$$\sqrt{I_{SHG}(T)} \propto d_{eff}(T) \propto \eta \tag{2}$$

The evolution of the order parameter η with temperature can be described by a simple critical power law derived from Landau theory:[35,52]

$$\eta = A\left(1 - \frac{T}{T_c}\right)^{\beta} \tag{3}$$

where A is a prefactor, T_c is the transition temperature, and β is the critical exponent.

Based on eqs 2 and 3, T_c and β values can be extracted from SHG results using

$$\eta = \sqrt{I_{SHG}(T)} = A\left(1 - \frac{T}{T_c}\right)^{\beta} \tag{4}$$

The fitting procedure performed from eq 4 with A, T_c, and β as free parameters returns upon cooling a β value of 0.255 ± 0.008 with T_c = 178.8 ± 0.3 K. Upon heating, β is 0.263 ± 0.008 with T_c = 179.1 ± 0.3 K (Figure 6). The experimental transition temperature (T_c: 178 K to 180 K) is thus consistent with the temperature determined by the fitting.

The order parameter η can also be obtained from XRPD by recording ψ (the angle between the molecular dipole C−F bond and the crystallographic a axis) versus temperature (see Figure 6). The XRPD data is fitted according to the power law (eq 4), in which A corresponds to $\psi_{(T\ 0K)}$ and gives rise to β = 0.250 ± 0.027 and T_c = 180.0 ± 0.1 K. It should be noticed here that the lowest temperature at which the structure was solved was 90 K, close to the temperature (92 K) at which reorientational motions are characterized by a relaxation time of the order of 100 s.[19] Below such temperature, reorientational motions are frozen, according to the previous dynamic study,[19] and thus, the LT phase becomes a low dimensional glass.[53−55] It is obvious that such a LT phase cannot be the stable phase at 0 K (the frozen disorder would confer a nonzero entropy) and the true stable phase remains, at present, elusive. Despite such thermodynamic evidence, for both TR SHG and ψ angle data from XRPD, we have assumed a continuous variation with temperature below 90 K and renormalization was performed under the hypothesis that the order parameter equals unity at 0 K. Under such assumptions, Figure 6 clearly shows that both TR SHG and the ψ angle from XRPD describe the second order transition.

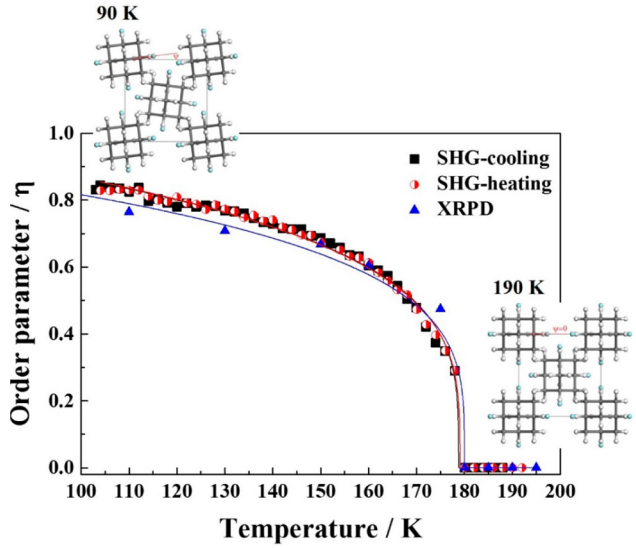

Figure 6. Order parameters determined from normalized values of the TR SHG data and the angle ψ between the C−F bond and the a (or b) crystallographic axis from XRPD. The black line corresponds to the fit of eq 4 for the TR SHG data on cooling (β is 0.255 ± 0.008 with T_c = 178.8 ± 0.3 K). The red line corresponds to the fit on heating (β is 0.263 ± 0.008 with T_c = 179.1 ± 0.3 K). The blue line corresponds to the fit of XRPD data (β is 0.250 ± 0.027 with T_c = 180.0 ± 0.1 K).

■ CONCLUSIONS

Phase transitions of 1 F A were thoroughly investigated by using TR SHG and XRPD. The combination of both techniques unveiled a new phase with a stability domain between 178 and 231 K. A second order transition occurs at 178 K between the LT phase ($P42_1c$) and the intermediate temperature phase (MT, $P4_2/nmc$), which arises from a continuous tilt of the molecules by thermal agitation. A first order transition occurs at 231 K between the MT phase and the high temperature cubic phase HT ($Fm3m$). Moreover, variation of the order parameter versus temperature for the second order transition was monitored by TR SHG and XRPD, and results are in good agreement to support the proposed second order transition mechanism.

In this work, the hint of a second order phase transition might arouse certain debate, as in the literature, for several compounds, second order transitions finally turned out to be first order transitions.[56] For instance, the undetectable thermal signature of theses transitions might be interpreted as inconsistent with thermodynamics. In fact, the structure differences between LT and MT phases are very subtle and the phase transition arises from a slight tilt of the 1 F A molecule. Neither lattice parameters nor volume show discontinuity at the transition temperature (178 K). Con sequently, transition between both phases should be difficult, even impossible, to be detected by usual DSC measurements. Measurement of heat capacity (C_p) at low temperature might give some indications of the MT ↔ LT transition. So, further

study of this second order transition combining other techniques could be suitable. For example, X ray absorption near edge structure (XANES) might provide certain information about the change of the local symmetry. Finally, this work underlines that the study of polymorphs and phase transitions should be carried out carefully. The combination of TR SHG and XRPD seems a suitable tool to monitor subtle symmetry changes when noncentrosymmetric structures are involved, such as, in diamondoids. In light of the present study, a thorough reinvestigation of phase transitions in adamantane derivatives could be envisaged.

■ AUTHOR INFORMATION

Corresponding Author

*E mail: gerard.coquerel@univ rouen.fr.

ORCID

Lina Yuan: 0000 0003 3687 2495

Valérie Dupray: 0000 0001 6188 0943

Notes

The authors declare no competing financial interest.

■ ACKNOWLEDGMENTS

This work was partially supported by the CICyT (Spain) Project FIS2011 24439, and by DGU (Catalonia) project 2014SGR00581.

■ REFERENCES

(1) McIntosh, G. C.; Yoon, M.; Berber, S.; Tománek, D. *Phys. Rev. B: Condens. Matter Mater. Phys.* **2004**, *70* (4), 45401.

(2) Dahl, J. E.; Liu, S. G.; Carlson, R. M. K. *Science* **2003**, *299* (5603), 96−99.

(3) Yang, W. L.; Fabbri, J. D.; Willey, T. M.; Lee, J. R. I.; Dahl, J. E.; Carlson, R. M. K.; Schreiner, P. R.; Fokin, A. A.; Tkachenko, B. A.; Fokina, N. A.; Meevasana, W.; Mannella, N.; Tanaka, K.; Zhou, X. J.; van Buuren, T.; Kelly, M. A.; Hussain, Z.; Melosh, N. A.; Shen, Z. X. *Science* **2007**, *316* (5830), 1460−1462.

(4) Wang, Y.; Kioupakis, E.; Lu, X.; Wegner, D.; Yamachika, R.; Dahl, J. E.; Carlson, R. M. K.; Louie, S. G.; Crommie, M. F. *Nat. Mater.* **2008**, *7* (1), 38−42.

(5) Guo, W.; Galoppini, E.; Gilardi, R.; Rydja, G. I.; Chen, Y. H. *Cryst. Growth Des.* **2001**, *1* (3), 231−237.

(6) Affouard, F.; Guinet, Y.; Denicourt, T.; Descamps, M. *J. Phys.: Condens. Matter* **2001**, *13* (33), 7237−7248.

(7) Bée, M.; Amoureux, J. P. *Mol. Phys.* **1983**, *48* (1), 63−79.

(8) Decressain, R.; Amoureux, J. P.; Carpentier, L.; Nagy, J. B. *Mol. Phys.* **1991**, *73* (3), 553−569.

(9) Ben Hassine, B.; Negrier, Ph.; Barrio, M.; Mondieig, D.; Massip, S.; Tamarit, J. Ll. *Cryst. Growth Des.* **2015**, *15* (8), 4149−4155.

(10) Negrier, Ph.; Barrio, M.; Romanini, M.; Tamarit, J. Ll.; Mondieig, D.; Krivchikov, A. I.; Kepinski, L.; Jezowski, A.; Szewczyk, D. *Cryst. Growth Des.* **2014**, *14* (5), 2626−2632.

(11) Negrier, Ph.; Barrio, M.; Tamarit, J. Ll.; Mondieig, D. *J. Phys. Chem. B* **2014**, *118* (32), 9595−9603.

(12) Clark, T.; Knox, T. M. O.; Mackle, H.; McKervey, M. A. *J. Chem. Soc., Faraday Trans. 1* **1977**, *73* (0), 1224.

(13) Kawai, N. T.; Gilson, D. F. R.; Butler, I. S. *Can. J. Chem.* **1991**, *69* (11), 1758−1765.

(14) Jaeger, G. *Arch. Hist. Exact Sci.* **1998**, *53* (1), 51−81.

(15) Amoureux, J. P.; Bee, M.; Sauvajol, J. L. *Acta Crystallogr., Sect. B: Struct. Crystallogr. Cryst. Chem.* **1982**, *38* (7), 1984−1989.

(16) Guinet, Y.; Sauvajol, J. L.; Muller, M. *Mol. Phys.* **1988**, *65* (3), 723−738.

(17) Amoureux, J. P.; Castelain, M.; Bee, M.; Benadda, M. D.; More, M. *Mol. Phys.* **1985**, *55* (1), 241−251.

(18) Bée, M.; Amoureux, J. P. *Mol. Phys.* **1983**, *50* (4), 585−602.

(19) Ben Hassine, B.; Negrier, Ph.; Romanini, M.; Barrio, M.; Macovez, R.; Kallel, A.; Mondieig, D.; Tamarit, J. Ll. *Phys. Chem. Chem. Phys.* **2016**, *18* (16), 10924−10930.

(20) Kurtz, S. K.; Perry, T. T. *J. Appl. Phys.* **1968**, *39* (8), 3798−3813.

(21) Dougherty, J. P.; Kurtz, S. K. *J. Appl. Crystallogr.* **1976**, *9*, 145−158.

(22) Franken, P. A.; Ward, J. F. *Rev. Mod. Phys.* **1963**, *35* (1), 23−39.

(23) Wanapun, D.; Kestur, U. S.; Kissick, D. J.; Simpson, G. J.; Taylor, L. S. *Anal. Chem.* **2010**, *82* (13), 5425−5432.

(24) Sutherland, R. L. *Handbook of Nonlinear Optics*, 2nd ed.; Marcel Dekker, Inc.: New York, 2003.

(25) Bloembergen, N. *Nonlinear Optics (World Scientific)*, 4th ed.; World Scientific Publishing: Singapore, 1996.

(26) Vogt, H. *Appl. Phys.* **1974**, *5* (2), 85−96.

(27) Vogt, H. *Phys. Status Solidi B* **1973**, *58* (2), 705−714.

(28) Clevers, S.; Simon, F.; Sanselme, M.; Dupray, V.; Coquerel, G. *Cryst. Growth Des.* **2013**, *13* (8), 3697−3704.

(29) Smilowitz, L.; Henson, B. F.; Asay, B. W.; Dickson, P. M. *J. Chem. Phys.* **2002**, *117* (8), 3789−3798.

(30) Smilowitz, L.; Henson, B. F.; Romero, J. J. *J. Phys. Chem. A* **2009**, *113* (35), 9650−9657.

(31) Hall, R. C.; Paul, I. C.; Curtin, D. Y. *J. Am. Chem. Soc.* **1988**, *110* (9), 2848−2854.

(32) Aktsipetrov, O. A.; Misuryaev, T. V.; Murzina, T. V.; Blinov, L. M.; Fridkin, V. M.; Palto, S. P. *Opt. Lett.* **2000**, *25* (6), 411−413.

(33) Bergman, J. G. *J. Am. Chem. Soc.* **1976**, *98* (4), 1054−1055.

(34) Clevers, S.; Rougeot, C.; Simon, F.; Sanselme, M.; Dupray, V.; Coquerel, G. *J. Mol. Struct.* **2014**, *1078*, 61−67.

(35) Steinbrener, S.; Jahn, I. R. *J. Phys. C: Solid State Phys.* **1978**, *11* (7), 1337−1349.

(36) Chemla, D. S. *Rep. Prog. Phys.* **1980**, *43* (10), 1191.

(37) Sutherland, R. L. *Handbook of Nonlinear Optic*, 2nd ed.; Marcel Dekker: New York, 2003.

(38) Miller, R. C. *Appl. Phys. Lett.* **1964**, *5* (1), 17−19.

(39) Donakowski, M. D.; Gautier, R.; Lu, H.; Tran, T. T.; Cantwell, J. R.; Halasyamani, P. S.; Poeppelmeier, K. R. *Inorg. Chem.* **2015**, *54* (3), 765−772.

(40) Yuan, L.; Clevers, S.; Couvrat, N.; Cartigny, Y.; Dupray, V.; Coquerel, G. *Chem. Eng. Technol.* **2016**, *39* (7), 1326−1332.

(41) Clevers, S.; Simon, F.; Dupray, V.; Coquerel, G. *J. Therm. Anal. Calorim.* **2013**, *112* (1), 271−277.

(42) Simon, F.; Clevers, S.; Gbabode, G.; Couvrat, N.; Agasse Peulon, V.; Sanselme, M.; Dupray, V.; Coquerel, G. *Cryst. Growth Des.* **2015**, *15* (2), 946−960.

(43) Simon, F.; Clevers, S.; Dupray, V.; Coquerel, G. *Chem. Eng. Technol.* **2015**, *38* (6), 971−983.

(44) Rietveld, H. M. *J. Appl. Crystallogr.* **1969**, *2* (2), 65−71.

(45) Spek, A. L. *Acta Crystallogr., Sect. D: Biol. Crystallogr.* **2009**, *65* (2), 148−155.

(46) Rao, C. N. R.; Rao, K. J. *Phase Transitions in Solids: An Approach to the Study of the Chemistry and Physics of Solids*; McGraw Hill: 1978.

(47) Boyd, G.; Kasper, H.; McFee, J. *IEEE J. Quantum Electron.* **1971**, *7* (12), 563−573.

(48) Boyd, R. W. *Nonlinear Optics*, 3rd ed.; Academic Press: Burlington, 2008; pp 1−67.

(49) Nye, J. F. *Physical Properties of Crystals: Their Representation by Tensors and Matrices*; Clarendon Press, 1985.

(50) Marder, S. R.; Sohn, J. E.; Stucky, G. D. *Materials for Nonlinear Optics: Chemical Perspectives*; American Chemical Society, 1991.
(51) Dmitriev, V. G.; Gurzadyan, G. G.; Nikogosyan, D. N.; Lotsch, H. K. V. *Handbook of Nonlinear Optical Crystals*; Springer Series in Optical Sciences; Springer Berlin Heidelberg: Berlin, Heidelberg, 1999; Vol. *64*.
(52) Bruins, D. E.; Garland, C. W. *J. Chem. Phys.* **1975**, *63* (10), 4139–4142.
(53) Romanini, M.; Barrio, M.; Capaccioli, S.; Macovez, R.; Ruiz Martin, M. D.; Tamarit, J. Ll. *J. Phys. Chem. C* **2016**, *120* (19), 10614–10621.
(54) Pérez, S. C.; Zuriaga, M.; Serra, P.; Wolfenson, A.; Negrier, Ph.; Tamarit, J. Ll. *J. Chem. Phys.* **2015**, *143* (13), 134502.
(55) Tripathi, P.; Mitsari, E.; Romanini, M.; Serra, P.; Tamarit, J.; Ll; Zuriaga, M.; Macovez, R. *J. Chem. Phys.* **2016**, *144* (16), 164505.
(56) Mnyukh, Y. *Fundamentals of Solid State Phase Transitions, Ferromagnetism and Ferroelectricity*; AuthorHouse, 2001.